

Effects of ultrasonic irradiation on the properties of coatings obtained by electroless plating and electro plating

F. Touyeras^{a,*}, J.Y. Hihn^a, X. Bourgoïn^a, B. Jacques^a, L. Hallez^a, V. Branger^b

^a *Laboratoire de Chimie des Matériaux et Interfaces, Université de Franche-Comté, 25030 Besançon Cedex, France*

^b *PSA Peugeot Citroën, Centre technique de Belchamp, 25420 Voujeaucourt, France*

Received 12 March 2004; accepted 8 June 2004

Available online 2 September 2004

Abstract

This paper deals with the effects of ultrasonic irradiation on electroless copper coating i.e. metallic deposition on non-conductive substrates and on electroplating on metallic substrates. Ultrasonic irradiation was both applied during activation (surface preparation for the electroless coating) and during plating steps in both cases. Several parameters were monitored, such as plating rates, practical adhesion, hardness, internal stress versus varying acoustic powers and frequencies. Optimum conditions for irradiation time, frequency and power were determined for each step. It appears clearly that ultrasound use affects deposit properties. Then, changes in the coating mechanisms can be discussed, and several parameters will be explored in this paper, to explain enhancement of deposit properties: increase in catalyst specific area, stirring dependence, surface energy evolution, dihydrogen desorption, structure of coating.

© 2004 Elsevier B.V. All rights reserved.

Keywords: Sonoelectrochemistry; Electroless coating; Electroplating; Internal stress

1. Introduction

Metallic coatings represent a very important part of the surface treatment industry and concern key sectors of the industry such as automobile or aeronautics. Needs are then important, from the point of view of improvement of the quality of the metallic layer and from that of the manufacturing processes. There are two possible methods in aqueous solutions, one using electric current and the other using a chemical donor of electron. The latter, called electroless plating, has long been used as an industrial process [1]. The applications of this technique are well known in the field of providing conductive or decorative coating on non-con-

ductive substrates, like polymer surfaces. Nevertheless, this technique exhibits a certain number of restrictions, especially the weakness of layer adhesion strength, causing poor reliability of the deposit. Previous works [2–6] have shown that ultrasonic irradiation yield interesting effects and that the plating rates and deposit properties can be improved considerably, especially if ultrasonic irradiation takes place during both activation and plating steps [5]. Better conditions for plating rate optimization consist in a very strong ultrasonic agitation (15 W) during the activation step (with a high value of the mass transfer coefficient) and a lower acoustic power (5 W) during the first five minutes of plating. Therefore, plating rates reach the value of upto $5.6 \mu\text{m h}^{-1}$. This value can be considered as important for this type of plating processes ($2.5 \mu\text{m h}^{-1}$ is an average rate in silent conditions). Furthermore these studies show that ultrasound irradiation also improves deposit adhesion strength by decreasing internal stress [4,5], and the

* Corresponding author. Address: Francis TOUYERAS—LCMI-IUT, BP 1559, 30, Avenue de l'Observatoire, 25 009 Besançon Cedex, France. Tel.: +33 381 666862; fax: +33 381 666858.

E-mail address: francis.touyeras@univ-fcomte.fr (F. Touyeras).

enhancement effect observed leads us to think that ultrasound may influence other mechanisms involved in copper deposition [5]. Nevertheless, the industrial process has recently been modified, and sensitization and activation grouped in a single step. To help this discussion, recent bibliographic developments were checked and described in detail in this paper [7]. Ultrasound influences during this single step are examined comparing water contact angles and previous XPS measurements. In this case, the actual deposit step is examined in terms of plating rates and adhesion strength, in presence or in absence of ultrasound, and with sensitization and activation grouped in a single step. Results were plotted as a function of mass transfer coefficients for 3 ultrasonic frequencies (300, 500 and 800 kHz).

The use of ultrasound in electrodeposition experienced a period of neglect until the 1980s when cleaning baths and ultrasonic probes became more available [8,9]. Consequently, there has been an upsurge of interest in the use of sonoelectrochemistry due to the fact that many plating characteristics could be modified by ultrasound, such as coating structure and morphology. Some parameters are identified to be more sensitive to ultrasound, such as internal stress and hardness distribution [8].

2. Experimental

2.1. Ultrasound generation and experimental apparatus

All experiments were performed with a 100 W high frequency generator from electronic service, at various ultrasonic frequencies: 300, 500 and 800 kHz, in a cell filled with 1000 ml bath. Sonication is produced parallel to the liquid surface and specimens hung up vertically. In order to determine precisely both ultrasound parameters and agitation-induced effects, characterization of exposure conditions was needed. Acoustic power transmitted to the liquid electrolyte was determined by calorimetry [10]. Mass transfer measurements were characterized by electro-diffusional method [11–13]. For this purpose, sonoelectrochemical voltammograms of the ferro–ferri cyanide reversible couple on a stationary Pt electrode were plotted. Work electrode is a platinum film (10 mm×20 mm) stuck on an epoxide sample, located in the same position as the test piece in the plating tank. A typical voltametric curve exhibits a sigmoidal current response yielding a signal plateau at mass transport limited potential. Only the steady state value is considered. Mass transfer coefficient k_d is calculated as follows:

$$k_d = \frac{i_{lim}}{nFC}$$

where i_{lim} : mass transport-limited current density (A/m^2); F : the Faraday constant (96,500 C); n : number

Table 1
Sensitization and activation procedure

Component	Concentration ($g\ l^{-1}$)
SnCl ₂	12 $g\ l^{-1}$
PdCl ₂	8 $g\ l^{-1}$
Immersion time: 2 min and 30 s	
Temperature: 27 °C	

Table 2
Electroless plating procedure

Component	Concentration ($g\ l^{-1}$)
Copper	2
Sodium hydroxyde	7.8
Formaldehyde	3
EDTA	35
Plating time: 60 min	
Temperature: 48 °C	

of electrons exchanged; C : concentration in electroactive species (mol/m^3).

2.2. Electroless processes

The non-conductive substrate used in all experiments consists of 50×10×1 mm epoxide resin plates. Before copper plating, the epoxide specimens were polished (600 grade), then cleaned with glycol ether aqueous solution for 5 min, conditioned in a solution of isopropyl alcohol triisopropanolamine for 2 min, sensitized and activated according to a SHIPPLEY commercial procedure. Operating conditions are presented in Tables 1 and 2.

2.3. Electroplating processes

For these experiments, brass substrate was covered with a nickel coating by electrolytic reduction. Plating time has been calculated in order to obtain a 10 μm thickness using the Faraday law: plating time = 35 min. The brass substrates used consist of 50×10×5 mm plates. Before metal plating, the samples needed a surface preparation described in Table 3.

3. Electroless plating on non-conductive substrates

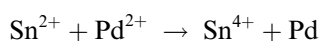
3.1. Electroless plating mechanisms

The previous preparation phase in two steps took place as follows [3,4]. During sensitization, active sites are produced by dipping the substrate in a reductive solution. SnCl₂ is a sensitizer because it favours nucleation and inlay of precious metallic catalyser particles. The sensitization bath usually contains SnCl₂ and

Table 3
Electroplating procedure

Step	Bath composition	Immersion time (min)	Temperature (°C)
Chemical cleaning	Alkaline bath: Presol 3500 at 50 g l ⁻¹	5	55
Electro cleaning	Alkaline bath: Presol 3500 at 50 g l ⁻¹	5	55
Activation	HCl 16%	5	Ambient
Plating	Watt bath: NiSO ₄ , 6H ₂ O at 250 g l ⁻¹ NiCl ₂ , 6H ₂ O at 45 g l ⁻¹ H ₃ BO ₃ at 30 g l ⁻¹ pH = 5 Brightener or not	35	55

chlorhydric acid. Some tin in a metallic form was added to the solution in order to avoid direct transformation of divalent tin ions into tetravalent tin. The activation step consists of providing catalysts. The substrate was immersed in a bath containing precious metal ions (usually palladium ions) and the global reaction is:



In this case, the sensitization and the activation steps can be carried out in a single step. In this case, the sensitization–activation step takes place using a Pd solution stabilized by a colloidal protective suspension composed of divalent Sn and Pd ions and chlorhydric acid. Some tetravalent Sn is added to facilitate hydrophobic substrate wettability. Reactions that occur and lead to the beginning of the copper coating can be illustrated by the following equilibria:

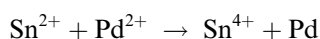
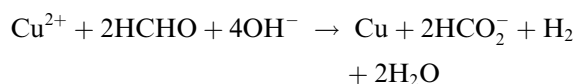


Fig. 1 shows the dissolution of tin palladium agglomerates in activation [6].

Palladium is needed at the substrate surface in order to reduce the Cu²⁺ ions. The higher the palladium surface concentration, the higher the plating rate. This

can be explained by the reactions that take place at the palladium surface: Fig. 2 [7].



A problem which may occur is the presence of dihydrogen [14,15]. During coating processes, water might be dissociated as follows:



The following reaction might occur:



Palladium plays a major role during the beginning of the coating. Hydrogen is adsorbed onto palladium in an ionic form, leading to the formation of active palladium in a metallic form. This adsorption decreases the presence of hydrogen in solution, and therefore decreases the competition between the reduction of copper and the reduction of hydrogen. This would lead to an increase in plating rate at the beginning of the deposit. At the same time, more copper nuclei would be formed on the surface by ultrasound, and mechanical anchoring of the copper in the fine pits on the resin surface would be favoured.

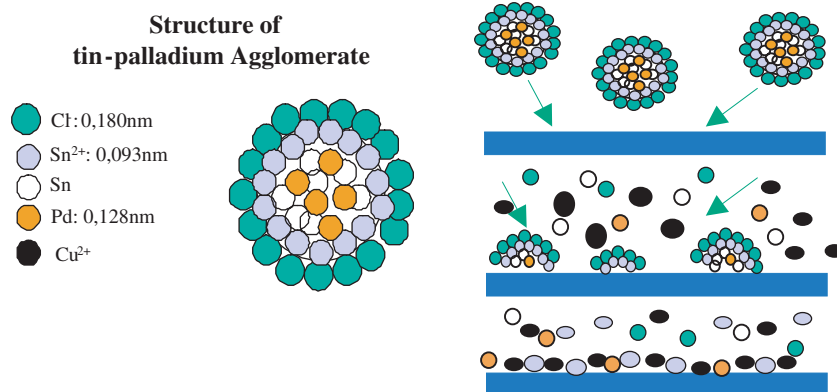


Fig. 1. Structure of the tin–palladium agglomerate and mechanism of dissolution. Particles with negative charges are adsorbed on the polymer surface.

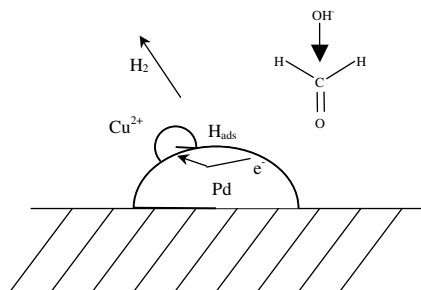


Fig. 2. Reactions at the palladium interface [4].

Applying ultrasound when the epoxide surface is fully covered with copper does not allow action on catalyst efficiency, and thus on the most important coating step. After this step, the effective catalyst area remains virtually unchanged and the plating rate constant.

3.2. Influence of ultrasonic irradiation on the activation step

The goal was to determine the effect of ultrasonic irradiation during the activation step on the palladium concentration at the sample surface. Some contact angle measurements were performed for three surface preparation conditions, and compared to previous XPS measurements [5].

The contact angle of epoxide plate and distilled water was measured with a Kruss angle-meter for different sample surface preparations [16]:

A: epoxide plate without surface preparation.

B: epoxide plate that undergoes the activation step without ultrasonic irradiation.

C: epoxide plate that undergoes the activation step with a 15 W ultrasonic irradiation.

The results are presented in Table 4.

The contact angle differences between surface preparation conditions A and B can be accounted for by the high palladium surface energy: during the activation step some palladium atoms are deposited at the epoxide surface, thus increasing sample surface energy and improving wettability. The contact angle decreases between B and C. It confirms XPS measurements [5]: epoxide specimen activated with ultrasound (15 W, 500 kHz) lead to a Pd atomic concentration of 2.69% as compared with 2.05% in silent conditions.

Table 4

Results of contact angle and palladium concentration on the epoxide surface as a function of the operating parameters

Sample	A	B	C
Contact angle (°)	61	44	22
Pd atomic concentration on epoxide surface measured by XPS (%)	0	2.05	2.69

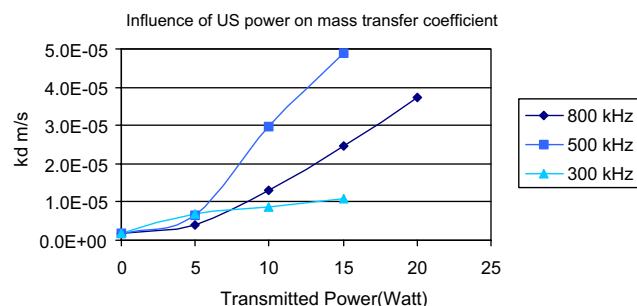


Fig. 3. Influence of ultrasonic transmitted power on mass transfer coefficient for different frequencies.

The mechanism involved is certainly a strong agitation, linked to very high values of mass transfer coefficient k_d , as this increases the catalyst area. In order to optimize the activation step operating conditions, i.e. highest stirring conditions, mass transfer coefficients were recorded versus transmitted power for different frequencies (300, 500 and 800 kHz).

Results shown in Fig. 3 confirm that mass transfer coefficient increases with transmitted ultrasonic power. This is true for each frequency, but the most important value is obtained for 500 kHz. The k_d value rises to around $5 \times 10^{-5} \text{ ms}^{-1}$ for 15 W of transmitted power.

3.3. Influence of ultrasonic irradiation on the plating step

Ultrasonic irradiation was applied during the first five minutes of the plating step whose sequence was found as optimum [4]. Measuring plating rate and practical adhesion versus mass transfer coefficient k_d shows a dependence in the same way for 500 kHz (Fig. 4). An optimum can be observed for k_d value of $1.25 \times 10^{-5} \text{ ms}^{-1}$ (corresponding to 5 W sonication), followed by a slight decrease when k_d increases. Minimum agitation is needed to ensure better dissolution of palladium agglomerate in alkaline media, but over strong turbulence may have a negative impact on metallic bonding formation. To complete this investigation, practical

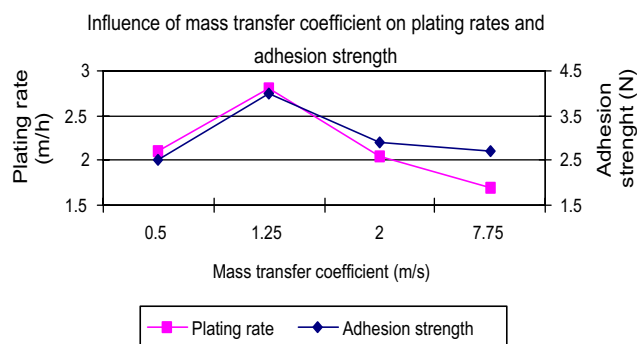


Fig. 4. Influence of mass transfer coefficient on plating rates and adhesion strength.

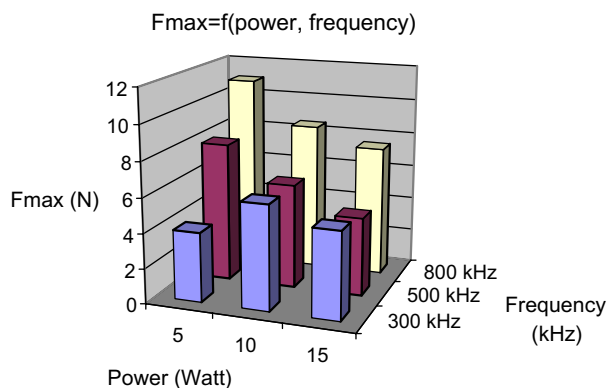


Fig. 5. Adhesion strength versus transmitted power and frequencies.

adhesion is measured as a function of ultrasonic power and frequency (Fig. 5). For a 500 and a 800 kHz frequency, practical adhesion varies in the same way with transmitted power: the lower the power, the higher adhesion strength, and 5 W is once again observed to be an optimal value. For 300 kHz, the maximal adhesion strength value is obtained for 10 W.

This influence of ultrasound during the plating step is more difficult to explain. Hydrogen degassing, which takes place simultaneously with metal deposition, can be involved. The amount of hydrogen occluded in the coating leads to porosity and tensile internal stress. Dihydrogen desorption of the plating substrate was evaluated with the gas carried method [14]. First results show the importance of hydrogen up to an amount of 0.35 ml in the copper coating (for a $50 \times 10 \text{ mm}^2$ sample with a 3 μm thickness). Unfortunately, values obtained under ultrasonic irradiation do not make it possible to establish an unambiguous tendency.

4. Electro plating on metallic substrates

Ultrasonic irradiation is applied using different frequencies (300, 500, and 800 kHz) and powers varying from 0 to 15 W during the plating step. Several effects are measured by monitoring final plating rate, deposit structure, internal stress and hardness.

4.1. Coating structure

Grain size varies as function of ultrasound power, for each frequency, and their distribution all along the sample is altered (Fig. 6). This is more visible when a brightener is used. For a 500 kHz frequency, an alternation of bright and mat areas alternation can be observed separated from each other by 1.5 mm. This length corresponds to a half wavelength. This observation was made in a previous work where such alternation was observed on silver plating in presence of organic brightener [17].

SEM pictures illustrate this, showing grain arrangements in the mat areas as though the deposit were made without ultrasound irradiation, with small, rounded and unorganised grains. In the bright areas, grains are organised in perpendicular lines to wave propagation direction. Grain size depends on ultrasonic power. This leads us to consider that mat areas correspond to pressure nodes. Without the help of a brightener, crystals have pyramidal forms and do not exhibit a privileged orientation, with low ultrasound influences.

Finally, ultrasonic irradiation does not modify deposit thickness, whether or not a brightener is used.

4.2. Internal stress measurements

Internal stress can be measured in two ways: the foil method and the X-ray diffraction method. In the former, a special sample with a reduced thickness (150 μm) is plated simultaneously with the other samples, one face hidden by a mask. The stress value is deduced from material bending after curvature measurement, when removing the mask, by the use of a theoretical model. Several model propositions are available in the literature. Arnyanaov [18,19] uses the same theoretical basis as Roche [20], but assumes that internal stress distribution is linear throughout thickness, in order to allow calculation by simple measurement of the foil curvature final value. As this point seems to be more adapted to the case of metallic coatings, it was chosen for this study.

The Arnyanaov model equation is as follows:

$$\sigma = -\frac{E_{\text{Cu}} h_{\text{Cu}}^2}{6h_{\text{Ni}} R(1 - \nu_{\text{Cu}})} \times \frac{1 + \gamma \theta^3}{1 + \theta}$$

R is the foil curvature, E the Young modulus, h the thickness, ν the Poisson coefficient, $\theta = \frac{h_{\text{Ni}}}{h_{\text{Cu}}}$ and

$$\gamma = \frac{E_{\text{Ni}}(1 - \nu_{\text{Cu}})}{(1 - \nu_{\text{Ni}})E_{\text{Cu}}}$$

The X-ray diffraction method is based on the determination of crystalline network elastic deformation. Internal stress is associated with the elastic theory. So, for a crystalline material, distances between two planes are clearly defined, and are characteristic of the material in a given metallurgic state. If the peak corresponding to the X-ray diffraction of a crystalline plane is slightly displaced, the new distances measured between two planes are linked to an internal stress modification.

So, values obtained by both methods versus ultrasonic powers are plotted in Fig. 7 for 500 kHz frequency. The influence of ultrasound is noticeable, and the global curve shape is the same for both measurement methods. However, values obtained by X-rays always remain higher than those obtained by foil curvature. This can be accounted for by the fact that measurement by X-rays only concerns the crystalline

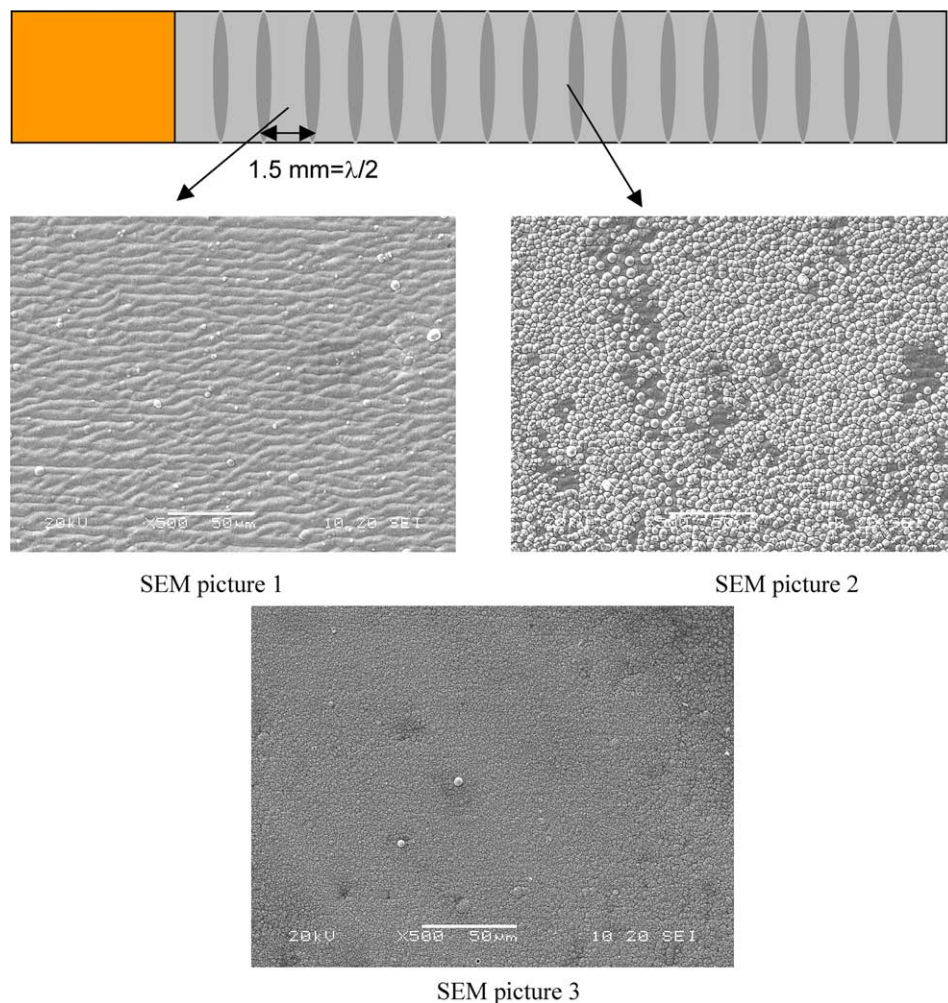


Fig. 6. Surface aspect of a coating realized under ultrasonic irradiation. Picture 1: ultrasonic irradiation at 500 kHz, with a brightener, bright area. Picture 2: ultrasonic irradiation at 500 kHz, with a brightener, mate area. Picture 3: silent conditions.

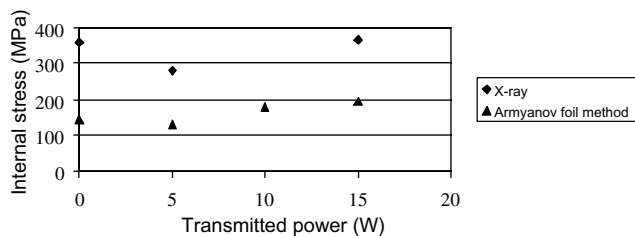


Fig. 7. Internal stress measured by X-ray and Arnyanaov methods versus transmitted power.

phase, and in our case the actual grains. On the contrary, the foil method includes the whole coating, taking into account amorphous zones. One can conclude that those amorphous zones are the location of internal stress relaxation, and that the grains are more sensible to ultrasonic irradiation. Once again, Fig. 7 shows that values are better for 5 W, especially for the X-ray method. In fact, amorphous zones seem to be less

numerous in silent conditions (see SEM pictures Fig. 6), leading to a large difference between global internal stress and internal stress in the grain, because relaxation usually takes place in these amorphous zones.

Hardness was measured with a micro-hardness HMV-M3 Shimadzu apparatus, and depends on ultrasound power and frequencies, and on brightener presence. At 500 kHz and with the use of a brightener, measurement of the hardness location on the sample surface shows a variation from 200 to 350 HV with a 1.5 mm step (Fig. 8). This is in accordance with visual and SEM observations, and the alternation of zones with different grains sizes can be directly linked to the hardness values.

For 800 kHz, the experimental results do not allow us to establish conclusions as clearly as for a 500 kHz frequency. Nevertheless the step is around 1 mm, which also corresponds to the half wavelength, but this scale is too small for a reliable resolution.

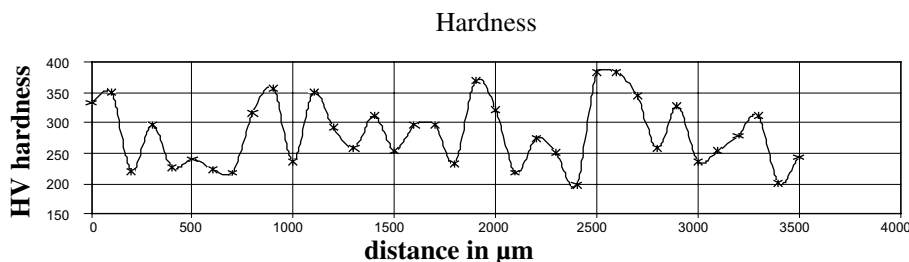


Fig. 8. Hardness profile in the wave propagation direction at 500 kHz and 15 W.

5. Conclusions

Ultrasound irradiation leads to a major modification of plating properties, for both electroless and electrolytic coatings. Many parameters are improved, such as plating rates and practical adhesion for electroless coating, but some mechanisms are not completely identified, and the ultrasound operating conditions are not completely controlled. A large effort has to be made from a technical point of view in ultrasound generation, particularly to erase the distribution effect on the sample surface.

At present we try to determinate internal stress rate all along the sample, with an accuracy of 1 mm with the X-ray method to establish a relationship between hardness and stress.

Acknowledgments

We would like to thank the CME (Centre de Microscopie Electronique) from the University of Franche-Comté for the SEM pictures, PSA Peugeot-Citroën for XPS and X-ray diffraction measurements, and NOV-ELECT (EDF) for financial help.

References

- [1] M. Paunovic, R. Arnd, *Journal of Electrochemical Science and Technology* 130 (4) (1983) 794.
- [2] R. Vasuaevan, R. Devanathan, K.D. Chidambaram, *Metal Finishing* 90 (10) (1992) 23.
- [3] Y. Zhao, C. Bao, R. Feng, Z. Chen, *Ultrasonics Sonochemistry* 2 (2) (1995) 99–103.
- [4] F. Touyeras, J.Y. Hihn, M.L. Doche, X. Roisard, *Ultrasonics Sonochemistry* 8 (2001) 285–290.
- [5] F. Touyeras, J.Y. Hihn, S. Delalande, R. Viennet, M.L. Doche, *Ultrasonics Sonochemistry* 10 (2003) 363–368.
- [6] R.L. Cohen, K.W. West, *Technologies Internationales* 80 (2002) 26–27.
- [7] O. Fouassier, Thesis, University of Bordeaux 1, 2001, pp. 116–117.
- [8] D.J. Walton, S.S. Phull, in: T.J. Mason (Ed.), *Advances in Sonochemistry*, vol. 4, JAI Press, London, 1996, p. 205.
- [9] R.G. Compton, J.C. Eklund, F. Marken, T.O. Rebbitt, R.P. Akkermans, D.N. Waller, *Electrochimica Acta* 42 (1997) 2919.
- [10] T.J. Mason, J.P. Lorimer, D.M. Bates, *Ultrasonics* 30 (1992) 40.
- [11] F. Trabelsi, H.A. Lyazidi, J. Berlan, P.L. Fabre, H. Delmas, A.M. Wilhelm, *Ultrasonics Sonochemistry* 3 (1996) 125.
- [12] E.L. Cooper, L.A. Coury, *Journal of Electrochemical Society* 145 (6) (1998) 1994–1999.
- [13] M.L. Doche, J.Y. Hihn, J.P. Lorimer, T.J. Mason, M. Plattes, *Ultrasonics Sonochemistry* 8 (2001) 291–298.
- [14] F. Cuevas, M. Hirscher, *Journal of Alloys and Compounds* 313 (1–2) (2000) 269–275.
- [15] S. Yamanaka, M. Fujikane, M. Uno, H. Murakami, O. Miura, *Journal of Alloys and Compounds* 366 (1–2) (2004) 264–268.
- [16] Y. Zhao, C. Bao, R. Feng, R. Li, *Plating and Surface Finishing* (1998) 98–100.
- [17] H.J. Wiesner, W.P. Frey, R.R. Vandervoort, E.L. Raymond, *Plating* 57 (4) (1970) 358–361.
- [18] S.A. Arnyanaov, *Metal Finishing* 91 (4) (1993) 59.
- [19] S.A. Arnyanaov, G. Sotirova-Chakarova, *Metal Finishing* 90 (11) (1992) 61–71.
- [20] A. Roche, *Revêtements et traitements de surface*, presses polytechniques universitaires romandes, 1998.